Research Article – Vol. 02, Issue 01, No. 05

Advanced in Engineering and Intelligence Systems

Journal Web Page: https://aeis.bilijipub.com

The optimal machine learning model for the precise prediction of high-performance concrete strength property

Yufeng Qian[1,*]

[1] *School of Science, Hubei University of Technology, Wuhan, 430068, China.*

Highlights

- Development of an optimal machine learning prediction models to evaluate high-performance concrete strength property
- Marine predator and grasshopper optimization algorithms are used for enhancing the accuracy of machine learning models
- The results of hybrid models show that the marine predator-based algorithm has better performance than grasshopper-based model
- The values of R2 for MPA-SVR and GOA-SVR are reported as 0.9939 and 0.9873.

Article Info

Received: 15 January 2023
Received in revised: 27 March 2023
Accepted: 12 March 2023
Available online: 28 March 2023

Keywords

compressive strength
high-performance concrete
marine predator algorithm
grasshopper optimization algorithm
support vector regression.

Abstract

The prominent mechanical property of concrete is compressive strength which guarantees the performance and safety of the structure in its life cycle. Assessment of compressive strength, especially for high-performance concrete, is first due to the nonlinear relationship between the compressive strength and the concrete constituents. Second, the supplementary cementitious materials admixed with the mix design of high-performance concrete encounter difficulties. The machine learning-based method, which relies on data mining, helps develop reliable and precise models to predict compressive strength. The present study employs a machine learning-based support vector regression (SVR) method to implement compressive strength prediction. The model accuracy was enhanced and strengthened by tuning the practical constraints of the support vector regression method. Marine predator and grasshopper optimization algorithms are performing the tuning process. The results of hybrid models show that the marine predator-based algorithm (MPA-SVR) played better than the grasshopper-based model (GOA-SVR) in predicting the compressive strength of high-performance concrete. The values of R^2 for MPA-SVR and GOA-SVR are reported as 0.9939 and 0.9873, which implies that the MPA-SVR is more capable of implementing the compressive strength prediction.

1. Introduction

In modern engineering structures, concrete covers a vast usage rate [1]. The difference in concrete mixtures provided modern concrete as high-performance concrete (HPC). HPC concrete is assumed as homogeneous concrete consisting of high-quality, cohesive materials, fine and coarse aggregates, and effective fine admixtures with a high rate of durability and workability [2], [3]. The usage of high-performance concrete is desired in the construction industry, such as houses, bridges, and other components, due to its positive effects on the reduction of concrete structure size, reducing the utilization of materials, increasing the durability of concrete, and the increment in the structures service life [4], [5]. The HPC concrete usually adds admixtures such as chemical, mineral, and fibrous material [6], [7].

The fly ash (FA) contains spherical-shaped glass beads, quartz, mullite, and a tiny number of inorganic

* Corresponding Author: Yufeng Qian
Email: yfqian@aliyun.com

crystals gathered from a coal-burning power plant flue [8]. The FA has pozzolanic feedback and rarely shows a self-hardening property. Moreover, the FA is a dust-like powder that replaces binder materials in the concrete mix design. Existing FA in the combination of the concrete has important effects on the concrete reaction and properties. For instance, its spherical shape facilitates the lubrication impact of the particle to cease segregation and bleeding and improves the workability of concrete. The FA pozzolanic feedback improves long-term compressive strength. Furthermore, the FA decreases the permeability of concrete due to its particle size leading to the enhancement of concrete persistence against diverse destructive environmental conditions and a structure with high density. Notably, the compressive strength of concrete with the FA mainly depends on the water to cement ratio, the amount of the FA, and the properties of other components combined in the concrete mix design [9]–[11].

Silica fume (SF) is utilized as a mineral admixture in the concrete mixture. This material is produced in the manufacturing process of silicon, ferrosilicon, and the most active pozzolanic ferroalloys [12], [13]. The pozzolanic reaction of the SF charges the concrete to show better bonding on the interface zone, especially in the paste aggregate of cement. Adding SF in concrete mix design is preferred to handle two tasks: filling the filler (mechanical aspect) and providing a high pozzolanic reaction in the concrete (chemical aspect). The pozzolanic reaction of SF in concrete helps form a secondary calcium silicate hydrate. This pozzolanic reaction of dust like SF is very prompt in the first seven days of concrete life, which causes enhancement of the short-term strength of concrete [3], [14], [15]. HPC concrete is a workable, durable, and highly abrasion-resistance concrete in which the water to cement ratio is low in its mixture and is cured perfectly [16]. The SF in the HPC concrete is preferred because of its extra-fine particle size and high pozzolanic feedback. Effects of the SF in the concrete are improved with the proper combination of superplasticizers where the amount of superplasticizer directly relates to the amount of the SF [17].

Table 1. the statistical features of variables applied in the hybrid models' development

Train										
Variables	B	FA	MS	SP	CA	TA	W	SP (%)	AGE	CS
Unite	(Kg/m^3)	(Kg/m^3)	(Kg/m^3)	(Kg/m^3)	(Kg/m^3)	(Kg/m^3)	(Kg/m^3)	(Kg/m^3)	(days)	(MPa)
Min	394	0	0	0	1086	1668	118.2	0	28	24
Max	500	275	43.3	13	1157	1867	205	13	180	106.3
Average	419.7458	97.84274	22.05508	4.562712	1132.602	1804.941	165.0525	4.562712	69.64407	64.4922
St. Deviation	41.1472	70.4681	17.7835	3.2628	24.8613	64.1614	28.2237	3.2628	49.3538	14.6519
Test										
Min	394	0	0	0	1086	1681	118.2	0	28	35.6
Max	500	225	43.3	10.5	1157	1867	205	10.5	180	107.8
Average	415.16	106.158	21.342	4.2576	1135.86	1807.78	167.02	4.2576	66.04	62.947
St. Deviation	37.850	53.0627	18.270	2.6705	23.3762	61.6329	30.0516	2.67059	51.8655	17.0076

Compressive strength is the significant factor that undertakes other properties of concrete and concrete structure safety. The most common way of assessing compressive strength is to perform physical and mechanical tests on the casting concrete. The other way is to use numerical simulations. In this method, the simplified form of materials is considered. The results are changed with the diverse forms of concrete structure discretization, which leads to random results. Using empirical regression models does not converge to accurate results due to the nonlinear relation between the compressive strength and the concrete constituents [18]–[20]. In recent years, machine learning-based methods have been widely applied in civil engineering[21]–[27]. These methods are mainly based on the dataset, and the method's accuracy is impressive of the sample set properties driven from literature. Some of these methods are artificial neural networks stochastic models [28]–[30], and other machine learning methods such as support vector regression (SVR) [31]and ensemble techniques [32]–[38]The shortage of these models is their black-box nature, which does not directly relate to the compressive strength and the concrete constituent variables. However, machine learning-based models serve as an accurate and healthy prediction of compressive strength.[39]–[45]

The present study focuses on adapting the support vector regression (SVR) method to predict compressive strength. The aim can be simplified in the accurate prediction of HPC compressive strength. A data set containing different combination designs of HPC is provided from the literature, including the FA, SF, and superplasticizer. The robustness of the SVR model is studied to be enhanced by two novel optimization algorithms; marine predator and grasshopper. The tuned

SVR models by the optimization algorithm are assessed by considering different evaluation metrics. Both models developed a precise prediction of HPC compressive strength. Finally, the best model is determined with the optimal structure.

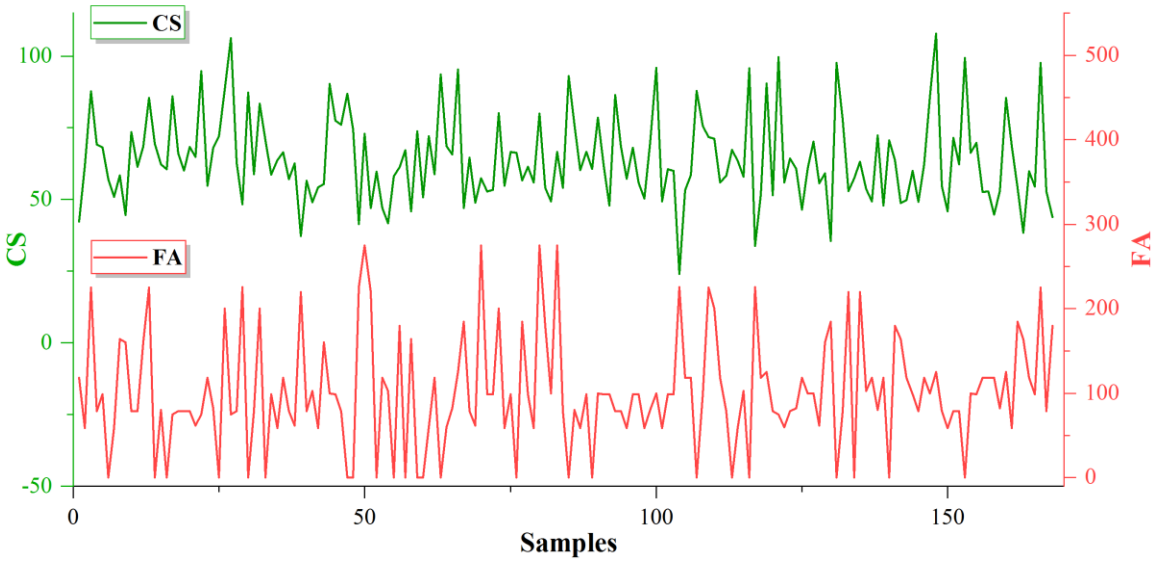

(a)

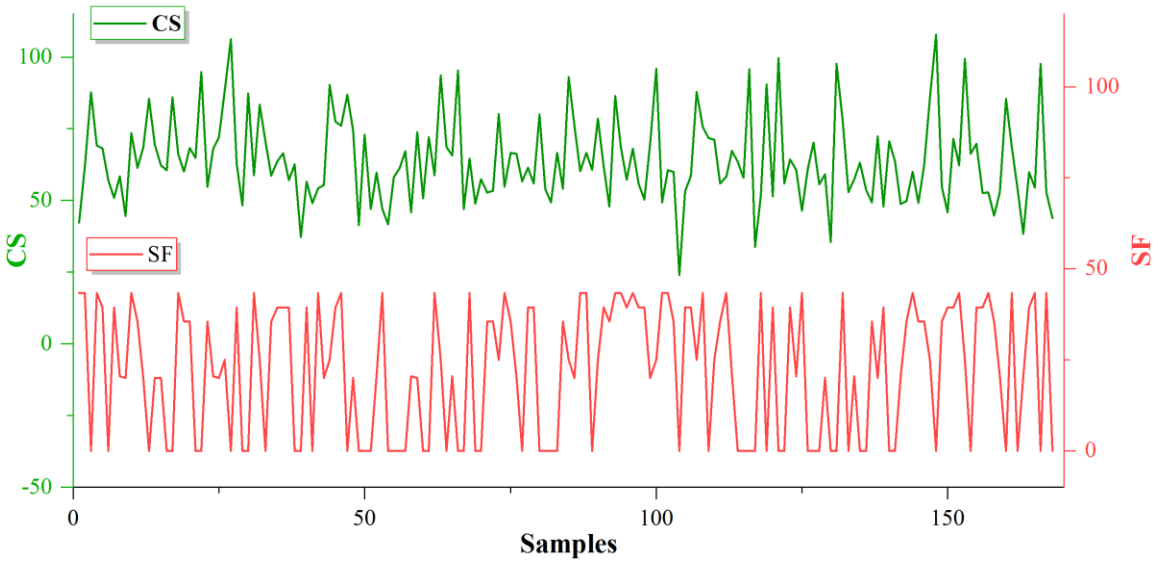

(b)

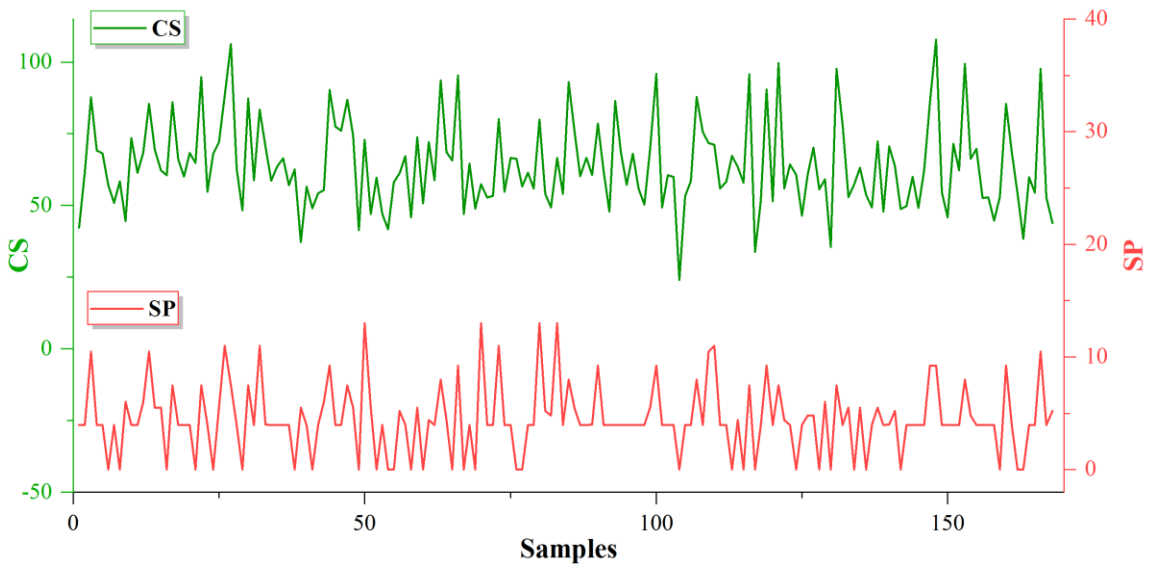

(c)

Fig. 1. admixtures applied in the high-performance concrete mix design to compressive strength: a) fly ash, b)silica fume, c) superplasticizer

2. Materials and methodology

2.1. Data collection

The dataset collected from the literature consists of 168 samples of different mix designs of HPC[46]. The mixed design applies to the mix design of the admixtures of fly ash, silica fume, and superplasticizer with various replacement percentages. The cement utilized in this data set is equal to ASTM type 1. The fly ash is of class F fly ash with low calcium equal to ASTM class F, and the silica fume is the condensed form of silica fume. The maximum and minimum fly ash and silica fume percentages are 0 to 55% and 0 to 5%, respectively. The coarse aggregate is crushed granite; the maximum size for mixes with water to cement ratio of 0.3 is 10 mm, and for the ratios of 0.4 and 0.5 is 20 mm. the dataset variables are fly ash (kg/m3), silica fume(kg/m3), superplasticizer (%), water (kg/m3), coarse aggregate (kg/m3), total aggregate(kg/m3), age (days) of concrete, cement (kg/m3) and the values of compressive strength (MPa). The range of admixtures and the related compressive strength are depicted in Fig.1. furthermore, the statistical properties of dataset variables are summarized in table 1.

2.2. Support vector regression (SVR)

The support vector machine (SVM) was primarily utilized for classification problems[47]. The regression form of SVM is the support vector regression (SVR) works by determining tolerance for regression displayed by ε. The ε defines the tolerance band, width. The SVR method is classified as a supervised learning technique that finds the best solution by an optimal hyper-plane process segregating the classification and regression phase of the method[48].

$$min_{w,b} = \frac{1}{2}\|\omega\|^2 + C\sum_{i=1}^{m}(\xi_i + \xi_i^*)$$
$$s.t. \quad \begin{Bmatrix} y_i - (\omega^T x_i + b) \le \varepsilon + \xi_i \\ (\omega x_i + b) - y_i \le \varepsilon + \xi_i^* \\ \xi_i, \xi_i^* \ge 0 \end{Bmatrix} \tag{1}$$

In the equation above ω is the indicator of weight and ξ the violation values of the boundary. b is the bias factor. ε and C define the deviation from the hyper-plane and regularization factors, respectively. In the fitness function of minimization, two terms are considered that carry different tasks

$\frac{1}{2}\|w\|^2$: in charge of increasing the distance between the hyper-plane and samples.

$C\sum_{i=1}^{m}(\xi_i + \xi_i^*)$: in charge of the adjuster's role of keeping the distance of the hyper-plane and samples to the lowest value of 1.

Its transition to a hyper-plane is implemented using a kernel function for a nonlinear dataset. The most applied kernel function is the quadratic kernel function [49]

$$K(x,y) = exp\,(-\gamma\|x-y\|^2) \tag{2}$$

$$\gamma = -1/2 \times sigma^2 \tag{3}$$

Hence, the parameters that tune an SVR model are ε and C and $sigma$. The determination of these parameters is effective in the accurate prediction of HPC.

2.3. *Marine predator algorithm (MPA)*

The marine predator algorithm is an innovative metaheuristic algorithm introduced by Faramrzi[50] et al. The predator employs an accepted foraging strategy, namely Brown and Levy random migration, in interacting with the prey. The Levy movement is for small prey, and the Brown is for highly focused prey. The Levy movement implements the exploration phase, which includes step-obeyed jumps. The BROWNIAN movement of step-fixed movement covers the exploitation phase. The predator's behavior is impressed by environmental factors such as aggregating devices of fish and eddy formation. The mathematical formulation of MPA is as follows.[51]

- The Brownian movement of prey, updating the Prey Matric:

$$\overrightarrow{step_j} = \overrightarrow{R_L} \otimes \left(\overrightarrow{Elite_j} - \left(\overrightarrow{R_L} \otimes \overrightarrow{prey_j}\right)\right) \quad (4)$$

$$\overrightarrow{prey_j} = \overrightarrow{prey_j} + \left(\overrightarrow{Elite_j} - \left(P.\vec{R} \otimes \overrightarrow{step_j}\right)\right) \quad (5)$$

Where R_L is a vector of a random number produced concerning Levy's movement. The other half of the agents are updated as follows:

$$\overrightarrow{step_j} = \overrightarrow{R_B} \otimes \left(\left(\overrightarrow{R_B} \otimes \overrightarrow{Elite_j}\right) - \overrightarrow{prey_j}\right) \quad (6)$$

$$\overrightarrow{prey_j} = \overrightarrow{Elite_j} + \left(P.cf \otimes \overrightarrow{step_j}\right) \quad (7)$$

Hence, the cf is defined as follows.

$$cf = \left[1 - \left(\frac{Iter}{Max} \times Iter\right)\right]^{\left(2.\frac{Iter}{Max} \times Iter\right)} \quad (8)$$

The Levy movement of predators and updating of the prey matrix is implemented as follows.

$$\overrightarrow{step_j} = \overrightarrow{R_L} \otimes \left(\left(\overrightarrow{R_L} \otimes \overrightarrow{Elite_j}\right) - \overrightarrow{prey_j}\right) \quad (9)$$

$$\overrightarrow{prey_j} = \overrightarrow{Elite_j} + \left(P.cf \otimes \overrightarrow{step_j}\right) \quad (10)$$

In each iteration, the elite matrix is updated with the best responses, and the final matrix after the last iteration is assumed as the final best solution. The flow chart of the MPA model is drawn in Fig.2.

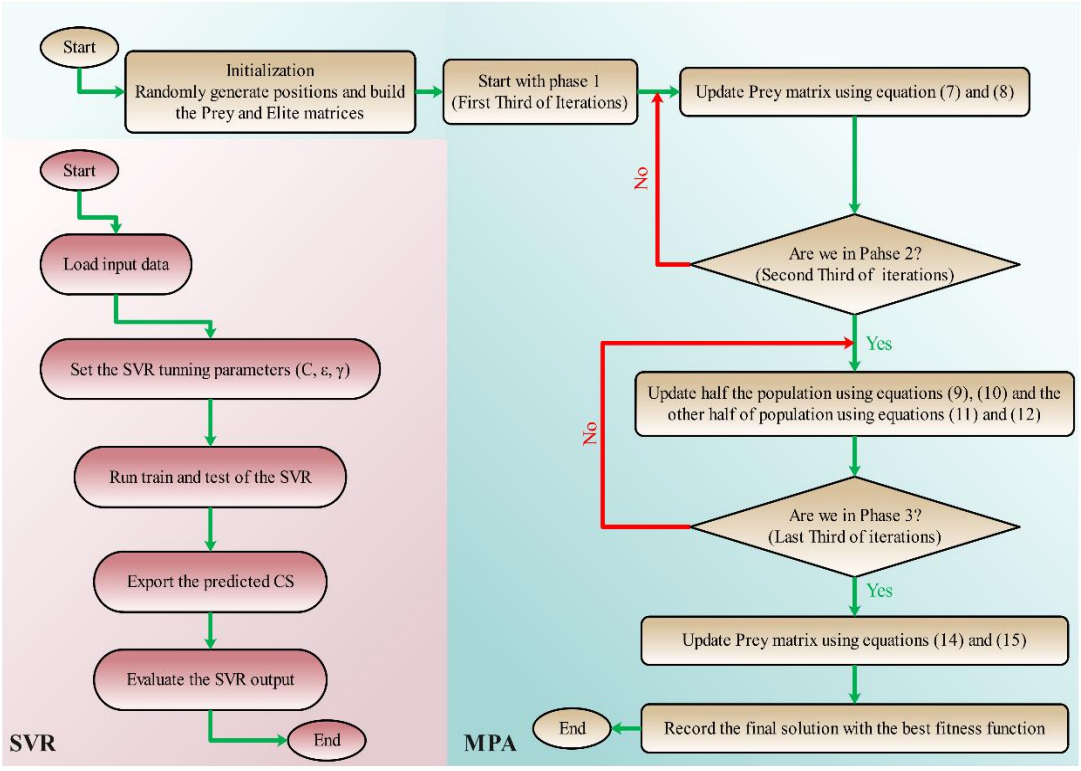

Fig. 2. the flowchart of hybrid marine predator-based support vector regression model.

2.4. Grasshopper optimization algorithm (GOA)

This algorithm simulates the grasshopper behavior to reach the best solution[52]. The grasshopper's life cycle starts from the egg, the nymph period, and at last, adulthood The swarm-based behavior of grasshoppers to path a long distance is trivial in adulthood. This long movement of grasshoppers has two features: long-range and abrupt movement. The mathematical formulation of these features is as follows.

$$x_i = S_i + G_i + A_i \tag{11}$$

where, x_i is the position of $i\,th$ grasshopper and S_i Defines the parameter that shows the social feedback of the grasshopper.

$$S_i = \sum_{\substack{j=1 \\ i\neq j}}^{N} s(d_{ij})\hat{d}_{ij} \ , \quad d_{ij} = |x_i - x_j| \ , \ \hat{d}_{ij} = \frac{x_i - x_j}{d_{ij}} \tag{12}$$

d_{ij} Indicates the space between $i\,th$ and $j\,th$ grasshopper. $\hat{d}_{ij}$ defines the unit vector between$i\,th$ and $j\,th$ grasshopper, and s is the strength of the social force.

$$s(x) = fe^{\frac{-x}{l}} - e^{-x} \tag{13}$$

In the above equation, f and l are the attraction intensity and length, respectively.

The direction of the wind is a prominent criterion of movement because the nymph grasshopper does not have wings.

$$A_i = u\hat{e}_w \ , \ G_i = -g\hat{e}_g \tag{14}$$

G_i and A_i defines the gravity force and wind advection of $i\,th$ grasshopper. $\hat{e}_w$ and $\hat{e}_g$ show the unit vector defining the direction of wind advection and the direction of gravity force. Moreover, u and g indicate the wind drift constant and the gravity constant, respectively. Assuming Eqs.12-14, Eq.11 can be changed as follows.

$$X_j^d = c\left[\sum_{\substack{j=1 \\ i\neq j}}^{N} c\frac{ub_d - lb_d}{2} s\left(\left|x_i^d - x_j^d\right|\right)\frac{x_i - x_j}{d_{ij}}\right] + \widehat{D}_d \tag{15}$$

Where ub_d and lb_d are the upper and lower boundary, $\widehat{D}_d$ is the $d\,th$ dimension value. N shows the population number, and c are reducing factors which, by increasing the iteration, helps balance the exploration and exploitation. This parameter is weighting the exploitation as the iteration goes up.

$$SCI = min\sum_{i=1}^{N}(C_i\,(P_{G_i}) - B_i(P_{D_i})) + C(P_{DGi}) \tag{16}$$

In this study, the values of c_{max} and c_{min} are assumed to be 1 and 0.0001, respectively.

2.5. Assessment of hybrid MPA-SVR and GOA-SVR models

the accuracy of models in the prediction of compressive strength and also the priority of models to each other is assessed considering some evaluation metrics such as coefficient of determination (R^2), root means square error (RMSE), mean absolute error (MAE), and variance account factor (VAF).

$$R^2 = \left(\frac{\sum_{n=1}^{N}(t_n - \bar{t})(p_n - \bar{p})}{\sqrt{[\sum_{n=1}^{N}(t_n - \bar{p})^2][\sum_{n=1}^{N}(p_n - \bar{p})^2]}}\right)^2 \tag{17}$$

$$RMSE = \sqrt{\frac{1}{N}\sum_{n=1}^{N}(t_n - p_n)^2} \tag{18}$$

$$MAE = \frac{1}{N}\sum_{n=1}^{N}|p_n - t_n| \tag{19}$$

$$VAF = \left(1 - \frac{var(t_n - p_n)}{var(t_n)}\right) * 100 \tag{20}$$

In the above equations, the desired value for R^2 is one and for other factors is zero. t_n and p_n show measured and predicted values of compressive strength, respectively.

Table 2. statistical evaluation results of hybrid proposed models

Metrics	Models			
	GOA-SVR		MPA-SVR	
	Train	Test	Train	Test
R2	0.9797	0.9873	0.9836	0.9939
RMSE	2.0845	1.9008	1.8821	1.3154
MAE	0.8587	0.677	0.6576	0.4959
VAF	97.8783	98.7311	98.2496	99.3944

3. Results and discussion

In this section, the models developed to predict compressive strength are being evaluated considering the mentioned metrics. The following subsection compares the hybrid models presented in this study.

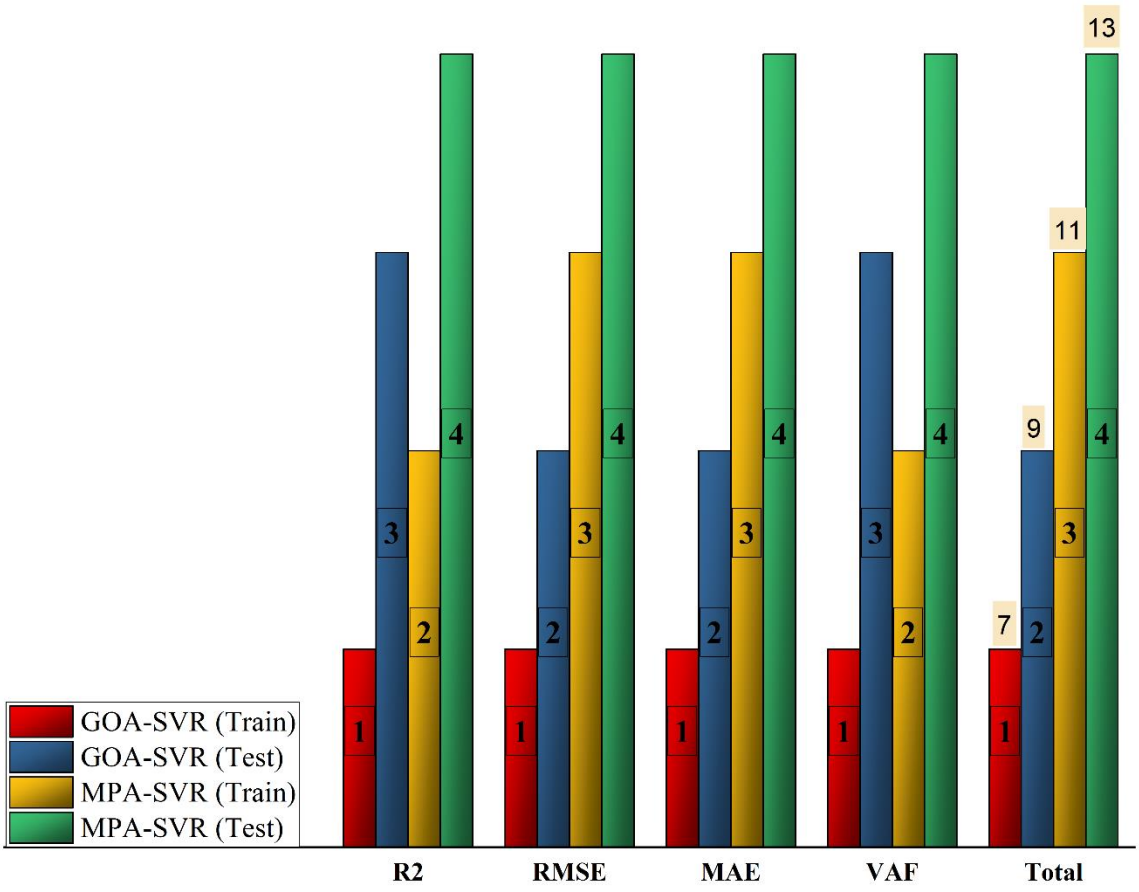

Fig. 3. considered a ranking system for the models to perform a comprehensive comparison

3.1.Models and data preparation

The models implement the prediction of compressive strength developed based on the SVR method. For this aim, the accuracy of models is enhanced by optimizing the structure of SVR. The tuning parameters mentioned for the SVR method are the prominent factors that strongly affect prediction accuracy. For this reason, the optimal determination of these key parameters is a significant matter in the prediction process of compressive strength. Two novel hybrid algorithms are presented to select the best SVR tuning parameters in the present study. The marine predator algorithm (MPA) model is called MPA-SVR, and the grasshopper optimization algorithm (GOA) based model is named GOA-SVR.

The coupling of the SVR model with GOA and MPA algorithm, which in Figs. 2, it is illustrated for the MPA-SVR model, are in a way that the SVR models as objective function receive the input and target variables. This function is called and tuned in each iteration by an optimization algorithm for C, ε, and γ. The RMSE values are assumed as the comparative criterion, and the maximum iteration number carries the stop point.

The dataset collected from the literature is tangibly illustrated in Fig.1 and table 1. The assessment of the model was performed in two phases of the training and testing, where about 70% of the data set with various samples of mixed design concerning the age of concrete was selected to develop the training phase, and 30% of the dataset was considered to validate the developed models. The input variables of models are considered non-dimensional by calculating their ratios in proportion to cement except for the Age and compressive strength values.

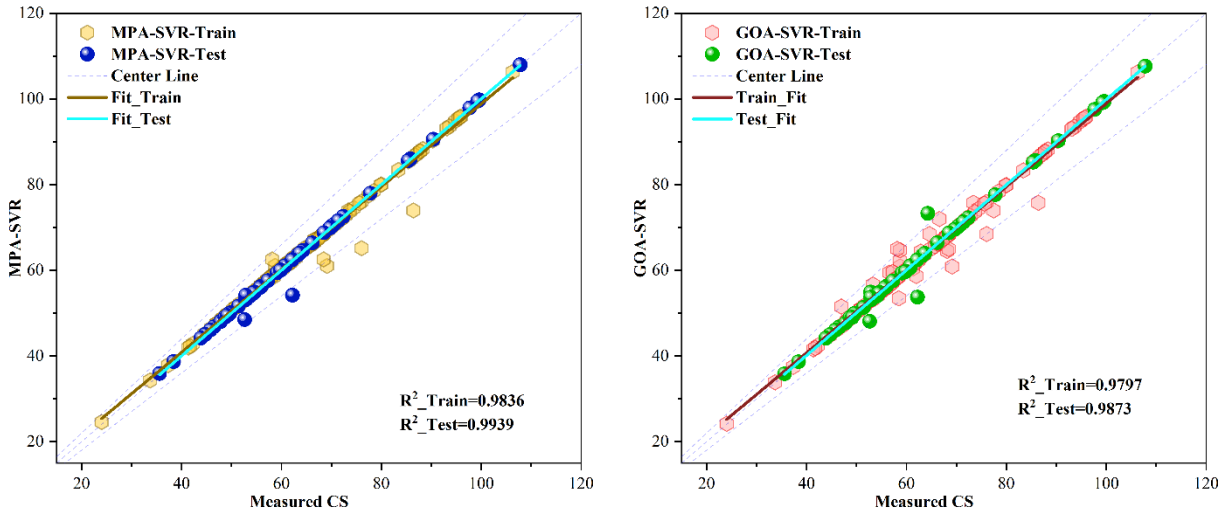

(a) (b)

Fig. 4. the scatter plot of the hybrid developed model: a) MPA-SVR b)GOA-SVR

3.2. Hybrid models assessment and discussion

The model's result based on the metrics is listed in table 2. The results for R^2 showed that the MPA-SVR model earned the best value for R^2 of 0.9939 in the training phase. The R^2 value in the training phase for the GOA-SVR model is 0.9873, which is a promising value. In the training phase, the value calculated for R^2 by the MPA-SVR model is higher than the GOA-SVR model, with 0.9836 and 0.9797, respectively. The model behavior in the case of RMSE value shows that the MPA-SVR model has proved 30 % enhancement compared to GOA-SVR in the test phase. The training phase also reported better values of RMSE for MPA-SVR than GOA-SVR by 1.8821 and 2.0845, respectively. Considering the MAE values in both models, the test phase shows better results than the training phase. The result clarifies that the MPA-SVR model also demonstrated better values than GOA-SVR. At last, the VAF values are improved with 98.7311 and 99.3944 in the test phase for GOA-SVR and MPA-SVR in the queue.

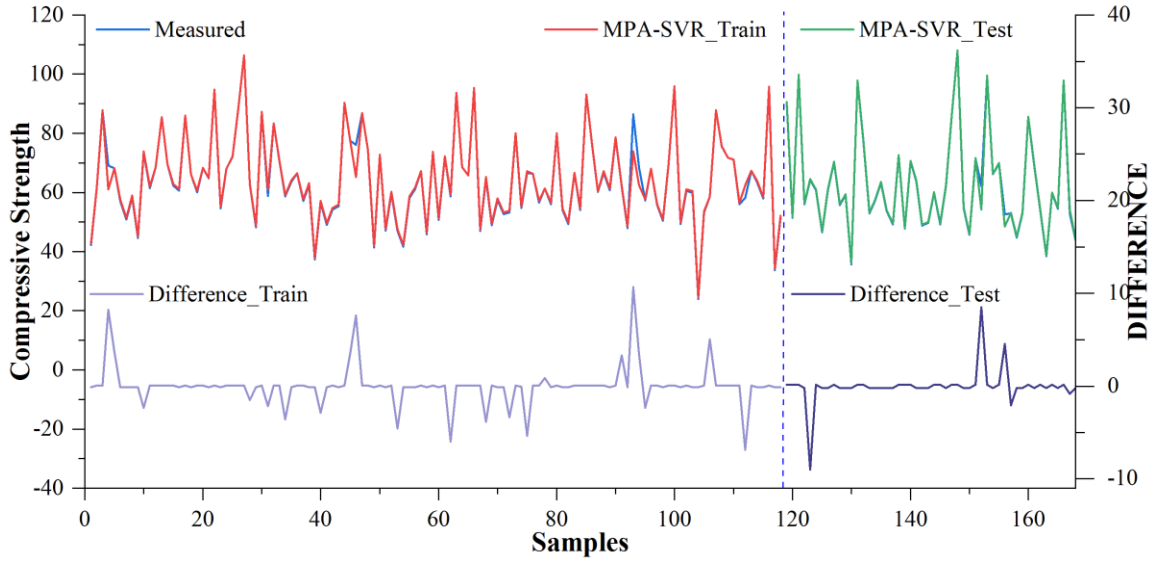

(a)

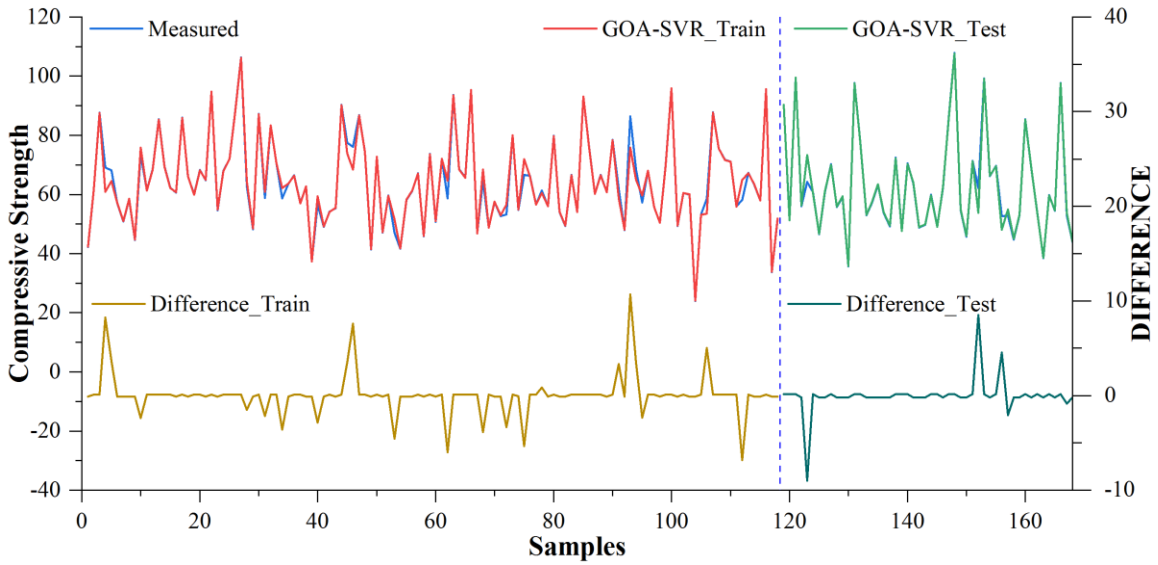

(b)

Fig. 5. time-series diagram of hybrid models and difference of predicted and measured values of compressive strength: a) MPA-SVR b)GOA-SVR

Fig .3 clarifies a ranking system to evaluate the model capability based on metrics results. The ranking system in terms of R^2 shows that the first and second-best values are for MPA –SVR model. for the RMSE, the ranking system defines the same trend as R^2. Furthermore, the values obtained for the MAE change the ranking system so that the first stage belongs to MPA-SVR, and the second is for the same model in the training phase. The third and fourth in terms of MAE are for the testing and the training phase of GOA-SVR, respectively. At last, the VAF ranking clarifies that the first stage with better values of the VAF is for the MPA-SVR model in the testing phase, and the last stage is for the GOA-SVR model in the training phase.

The scatter plot in Fig.4 illustrates the regression between the measured values of compressive strength and the predicted values of models. As shown in Fig.4, the accuracy of the MPA-SVR and GOA-SVR models in the train and the test phases are presented. The fitted lines for the values predicted by this model in the training and testing phase and the accommodation rate of these lines with the center line demonstrate the accurate prediction capability. It is clear from Fig.4 that the fitted line for the testing phase is in more accordance with the center line compared to the line fitted for the GOA-SVR model in the test phase. Also, considering the fitted lines for the training phase in both models relies on the fact that the training phase of the MPA-SVR model also serves a better match with the center line, which demonstrates higher accuracy of the MPA-SVR model to GOA-SVR model.

The dashed lines depicted in Fig.4 indicate the ±10 % deviation of the predicted value of compressive strength. Considering this fact, the observed deviation for the MPA-SVR model has occurred for samples less than 4. This deviation occurs in about 7 samples for the GOA-SVR model, which highlights the healthy prediction of the MPA-SVR model

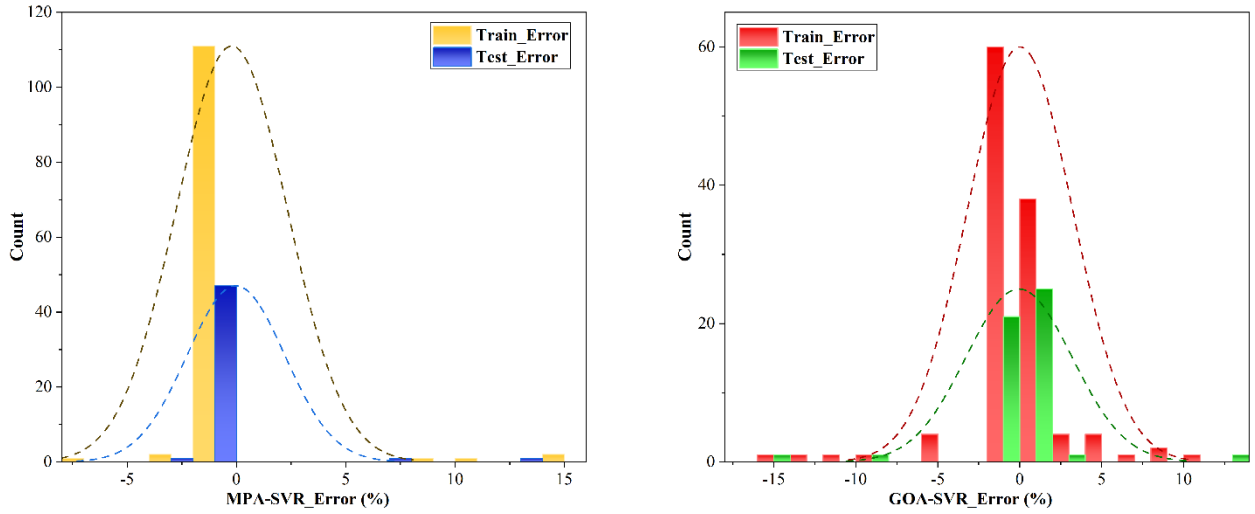

(a) (b)

Fig. 6. the error histogram of hybrid models: a) MPA-SVR b)GOA-SVR

The figure shows the time series distributions of measured compressive strength and the predicted values of models in Fig.5. the difference between measured and predicted values are also provided. The distribution of compressive values and the predicted values for the MPA-SVR are in good agreement and serve the best accordance in the time series. This behavior is valid for the GOA-SVR model with lower accuracy than the MPA-SVR model. Also, considering the difference of predicted values by both models and the measured values, the difference is partially identical, with little variation in the deviation between the predicted and measured compressive strength, where the rate of these varieties is higher for GOA-SVR than for MPA-SVR.

Furthermore, the histogram and related distribution are presented in Fig.6. The density of error percentage is understandable in this figure. As shown, for the MPA-SVR model, the error percentage is condensed to the range of error less than 5%, which can be concluded that the model has predicted the compressive strength with approximately 5% confidence. Moreover, the maximum error reported for the MPA-SVR model is less than 15%. The same histogram is depicted for the GOA-SVR model, where the error is accumulated in the range of 5%. However, error congestion is also detectable out of the 5% range. The maximum error recorded for this model is higher than the MPA-SVR model and heats more than 15 % values.

4. Conclusion

The prominent mechanical property of concrete is compressive strength which guarantees the performance and safety of the structure in its life cycle. Assessment of compressive strength, especially for the HPC, first due to the nonlinear relationship between the compressive strength and the concrete constituents and second for the supplementary cementitious materials that are admixed to the mix design of HPC, has encountered difficulties. The machine learning-based method helps develop reliable and precise models to predict compressive strength. In the present study, a machine learning-based regression method, support vector regression employed to implement the prediction of compressive strength. The model accuracy is enhanced and strengthened by tuning the effective constraints of the SVR method, which is performed by MPA and GOA algorithms. A data set of HPC collected from literature with admixtures such as FA, MS, and SP was considered to feed the models. Models output is evaluated with statistical metrics to have a perfect comparison between two tune models and show the robustness of models in predicting compressive strength. The results obtained from the models showed that the MPA-SVR model has delivered more acceptable results than the GOA-SVR model. the results considering the R^2 values imply that the MPA-SVR model has presented better values compared to GOA-SVR. Also, the MPA-SVR model showed a 20 % improvement in RMSE values to GOA-SVR. The

comprehensive study of two developed models reveals that both models have an acceptable prediction of compressive strength. However, the MPA-SVR model demonstrated a promising, flexible, and robust prediction of compressive strength.

Acknowledgments

This paper is supported by the guiding project B2019048 of the Science and Technology Research Plan of the Education Department of Hubei Province: Theoretical research on the Stability of Complex Networks.

REFERENCES

[1] V. Afroughsabet, L. Biolzi, and T. Ozbakkaloglu, "High-performance fiber-reinforced concrete: a review," *J Mater Sci*, vol. 51, pp. 6517–6551, 2016.

[2] S. Fallah and M. Nematzadeh, "Mechanical properties and durability of high-strength concrete containing macro-polymeric and polypropylene fibers with nano-silica and silica fume," *Constr Build Mater*, vol. 132, pp. 170–187, Feb. 2017, doi: 10.1016/j.conbuildmat.2016.11.100.

[3] M. Nematzadeh and S. Fallah-Valukolaee, "Effectiveness of fibers and binders in high-strength concrete under chemical corrosion," *Structural engineering and mechanics: An international journal*, vol. 64, no. 2, pp. 243–257, 2017.

[4] H. Jafarzadeh and M. Nematzadeh, "Evaluation of post-heating flexural behavior of steel fiber-reinforced high-strength concrete beams reinforced with FRP bars: Experimental and analytical results," *Eng Struct*, vol. 225, p. 111292, Dec. 2020, doi: 10.1016/j.engstruct.2020.111292.

[5] M. Nematzadeh, S.-A. Hosseini, and T. Ozbakkaloglu, "The combined effect of crumb rubber aggregates and steel fibers on shear behavior of GFRP bar-reinforced high-strength concrete beams," *Journal of Building Engineering*, vol. 44, p. 102981, Dec. 2021, doi: 10.1016/j.jobe.2021.102981.

[6] P. Zhang, C. Liu, and Q. Li, "Application of Gray Relational Analysis for Chloride Permeability and Freeze-Thaw Resistance of High-Performance Concrete Containing Nanoparticles," *Journal of Materials in Civil Engineering*, vol. 23, no. 12, pp. 1760–1763, Dec. 2011, doi: 10.1061/(ASCE)MT.1943-5533.0000332.

[7] Y. Meng *et al.*, "Effect of geopolymer as an additive on the mechanical performance of asphalt," *Road Materials and Pavement Design*, pp. 1–20, Sep. 2021, doi: 10.1080/14680629.2021.1977169.

[8] S. W. M. Supit and F. U. A. Shaikh, "Durability properties of high volume fly ash concrete containing nano-silica," *Mater Struct*, vol. 48, no. 8, pp. 2431–2445, Aug. 2015, doi: 10.1617/s11527-014-0329-0.

[9] M. Jalal, A. Pouladkhan, O. F. Harandi, and D. Jafari, "RETRACTED: Comparative study on effects of Class F fly ash, nano silica and silica fume on properties of high-performance self-compacting concrete," *Constr Build Mater*, vol. 94, pp. 90–104, Sep. 2015, doi: 10.1016/j.conbuildmat.2015.07.001.

[10] P. R. de Matos, M. Foiato, and L. R. Prudêncio, "Ecological, fresh state and long-term mechanical properties of high-volume fly ash high-performance self-compacting concrete," *Constr Build Mater*, vol. 203, pp. 282–293, Apr. 2019, doi: 10.1016/j.conbuildmat.2019.01.074.

[11] R. Siddique, "Properties of self-compacting concrete containing class F fly ash," *Mater Des*, vol. 32, no. 3, pp. 1501–1507, Mar. 2011, doi: 10.1016/j.matdes.2010.08.043.

[12] H. Asgeirsson, "Silica fume in cement and silane for counteracting of alkali-silica reactions in iceland," *Cem Concr Res*, vol. 16, no. 3, pp. 423–428, May 1986, doi: 10.1016/0008-8846(86)90118-3.

[13] S. Chatterji, N. Thaulow, and P. Christensen, "Puzzolanic activity of byproduct silica-fume from ferro-silicom production," *Cem Concr Res*, vol. 12, no. 6, pp. 781–784, Nov. 1982, doi: 10.1016/0008-8846(82)90042-4.

[14] W. Liao, X. Sun, A. Kumar, H. Sun, and H. Ma, "Hydration of Binary Portland Cement Blends Containing Silica Fume: A Decoupling Method to Estimate Degrees of Hydration and Pozzolanic Reaction," *Front Mater*, vol. 6, Apr. 2019, doi: 10.3389/fmats.2019.00078.

[15] M. Á. Sanjuán, C. Argiz, J. C. Gálvez, and A. Moragues, "Effect of silica fume fineness on the improvement of Portland cement strength performance," *Constr Build Mater*, vol. 96, pp. 55–64, Oct. 2015, doi: 10.1016/j.conbuildmat.2015.07.092.

[16] N. De Belie, M. Soutsos, and E. Gruyaert, *Properties of fresh and hardened concrete containing supplementary cementitious materials*, vol. 25. Springer, 2018.

[17] K. Kovler and N. Roussel, "Properties of fresh and hardened concrete," *Cem Concr Res*, vol. 41, no. 7, pp. 775–792, Jul. 2011, doi: 10.1016/j.cemconres.2011.03.009.

[18] F. Khademi, M. Akbari, and S. M. Jamal, "Prediction of compressive strength of concrete by data-driven models," *I-Manager's J Civ Eng*, vol. 5, pp. 16–23, 2015.

[19] P. Zhang, Z. Gao, J. Wang, and K. Wang, "Numerical modeling of rebar-matrix bond behaviors of nano-SiO2 and PVA fiber reinforced geopolymer composites," *Ceram Int*, vol. 47, no. 8, pp. 11727–11737, Apr. 2021, doi: 10.1016/j.ceramint.2021.01.012.

[20] D. J. Armaghani and P. G. Asteris, "A comparative study of ANN and ANFIS models for the prediction of cement-based mortar materials compressive strength," *Neural Comput Appl*, vol. 33, no. 9, pp.

4501–4532, May 2021, doi: 10.1007/s00521-020-05244-4.
[21] F. Masoumi, S. Najjar-Ghabel, A. Safarzadeh, and B. Sadaghat, "Automatic calibration of the groundwater simulation model with high parameter dimensionality using sequential uncertainty fitting approach," *Water Supply*, vol. 20, no. 8, pp. 3487–3501, 2020.
[22] S. Kumar and S. Robinson, "Estimating the Pile Settlement Using a Machine Learning Technique Optimized by Henry's Gas Solubility Optimization and Particle Swarm Optimization," *Advances in Engineering and Intelligence Systems*, vol. 1, no. 04, 2023.
[23] A. Sieck and G. Daniels, "Utilizing the Novel developed MLP Techniques to Survey Pile Subsidence via Optimization Algorithms," *Advances in Engineering and Intelligence Systems*, vol. 1, no. 03, 2022.
[24] D. Cadasse and A. Fontana, "Advanced in Engineering and Intelligence Systems," 2022.
[25] N. Zhangabay, "Evaluate The Depth of Scouring of the Bridge Base Using Soft Calculation Techniques," *Advances in Engineering and Intelligence Systems*, vol. 1, no. 02, 2022.
[26] H. Cheng, S. Kitchen, and G. Daniels, "Novel hybrid radial based neural network model on predicting the compressive strength of long-term HPC concrete," *Advances in Engineering and Intelligence Systems*, vol. 1, no. 02, 2022.
[27] N.-B. Chang, U. Hossain, A. Valencia, J. Qiu, and N. Kapucu, "The role of food-energy-water nexus analyses in urban growth models for urban sustainability: A review of synergistic framework," *Sustain Cities Soc*, vol. 63, p. 102486, 2020.
[28] M. Słoński, "A comparison of model selection methods for compressive strength prediction of high-performance concrete using neural networks," *Comput Struct*, vol. 88, no. 21–22, pp. 1248–1253, Nov. 2010, doi: 10.1016/j.compstruc.2010.07.003.
[29] S. Lai and M. Serra, "Concrete strength prediction by means of neural network," *Constr Build Mater*, vol. 11, no. 2, pp. 93–98, 1997.
[30] H.-G. Ni and J.-Z. Wang, "Prediction of compressive strength of concrete by neural networks," *Cem Concr Res*, vol. 30, no. 8, pp. 1245–1250, 2000.
[31] M. Słoński, "A comparison of model selection methods for compressive strength prediction of high-performance concrete using neural networks," *Comput Struct*, vol. 88, no. 21–22, pp. 1248–1253, 2010.
[32] K. Yan and C. Shi, "Prediction of elastic modulus of normal and high strength concrete by support vector machine," *Constr Build Mater*, vol. 24, no. 8, pp. 1479–1485, 2010.
[33] Q. Han, C. Gui, J. Xu, and G. Lacidogna, "A generalized method to predict the compressive strength of high-performance concrete by improved random forest algorithm," *Constr Build Mater*, vol. 226, pp. 734–742, 2019.
[34] D.-C. Feng *et al.*, "Machine learning-based compressive strength prediction for concrete: An adaptive boosting approach," *Constr Build Mater*, vol. 230, p. 117000, 2020.
[35] H. I. Erdal, O. Karakurt, and E. Namli, "High performance concrete compressive strength forecasting using ensemble models based on discrete wavelet transform," *Eng Appl Artif Intell*, vol. 26, no. 4, pp. 1246–1254, 2013.
[36] U. Anyaoha, A. Zaji, and Z. Liu, "Soft computing in estimating the compressive strength for high-performance concrete via concrete composition appraisal," *Constr Build Mater*, vol. 257, p. 119472, 2020.
[37] J.-S. Chou, C.-K. Chiu, M. Farfoura, and I. Al-Taharwa, "Optimizing the prediction accuracy of concrete compressive strength based on a comparison of data-mining techniques," *Journal of Computing in Civil Engineering*, vol. 25, no. 3, pp. 242–253, 2011.
[38] M. H. Rafiei, W. H. Khushefati, R. Demirboga, and H. Adeli, "Supervised deep restricted Boltzmann machine for estimation of concrete," *ACI Mater J*, vol. 114, no. 2, p. 237, 2017.
[39] B. A. Young, A. Hall, L. Pilon, P. Gupta, and G. Sant, "Can the compressive strength of concrete be estimated from knowledge of the mixture proportions?: New insights from statistical analysis and machine learning methods," *Cem Concr Res*, vol. 115, pp. 379–388, 2019.
[40] T. Le-Duc, Q.-H. Nguyen, and H. Nguyen-Xuan, "Balancing composite motion optimization," *Inf Sci (N Y)*, vol. 520, pp. 250–270, 2020.
[41] M. Engen *et al.*, "Predictive strength of ready-mixed concrete: Exemplified using data from the Norwegian market," *Structural Concrete*, vol. 19, no. 3, pp. 806–819, 2018.
[42] B. Das, V. Mukherjee, and D. Das, "Student psychology based optimization algorithm: A new population based optimization algorithm for solving optimization problems," *Advances in Engineering software*, vol. 146, p. 102804, 2020.
[43] A. Dey, G. Miyani, and A. Sil, "Application of artificial neural network (ANN) for estimating reliable service life of reinforced concrete (RC) structure bookkeeping factors responsible for deterioration mechanism," *Soft comput*, vol. 24, pp. 2109–2123, 2020.
[44] A. Falih and A. Z. M. Shammari, "Hybrid constrained permutation algorithm and genetic algorithm for process planning problem," *J Intell Manuf*, vol. 31, pp. 1079–1099, 2020.
[45] J.-S. Chou, W. K. Chong, and D.-K. Bui, "Nature-inspired metaheuristic regression system: programming and implementation for civil engineering applications," *Journal of Computing in Civil Engineering*, vol. 30, no. 5, p. 04016007, 2016.
[46] L. Lam, Y. L. Wong, and C.-S. Poon, "Effect of fly ash

and silica fume on compressive and fracture behaviors of concrete," *Cem Concr Res*, vol. 28, no. 2, pp. 271–283, 1998.
[47] L. Wang, *Support vector machines: theory and applications*, vol. 177. Springer Science & Business Media, 2005.
[48] V. Vapnik, *The nature of statistical learning theory*. Springer science & business media, 1999.
[49] A. Faramarzi, M. Heidarinejad, S. Mirjalili, and A. H. Gandomi, "Marine Predators Algorithm: A nature-inspired metaheuristic," *Expert Syst Appl*, vol. 152, p. 113377, 2020.
[50] M. Ramezani, D. Bahmanyar, and N. Razmjooy, "A new improved model of marine predator algorithm for optimization problems," *Arab J Sci Eng*, vol. 46, no. 9, pp. 8803–8826, 2021.
[51] M. Saremi, "Lewis, 2017 Saremi S., Mirjalili S., Lewis A," *Grasshopper optimisation algorithm: Theory and application, Advances in Engineering Software*, vol. 105, pp. 30–47, 2017.
[52] S. M. Rogers, T. Matheson, E. Despland, T. Dodgson, M. Burrows, and S. J. Simpson, "Mechanosensory-induced behavioural gregarization in the desert locust Schistocerca gregaria," *Journal of Experimental Biology*, vol. 206, no. 22, pp. 3991–4002, 2003.